International Journal of Emerging Information Science and Technology Vol. 6, No. 1, (2025), pp. 32-41

Performance of Long Range-Frequency Hopping Spread Spectrum (LR-FHSS) For LoRaWAN Satellite Communication

Puput Dani Prasetyo Adi[1], Kevin Stekelorom [2]

[1]National Research and Innovation Agency (BRIN), Indonesia
[2]University Polytechnic Hauts-De-France, Valenciennes, France

Email: [1,]pupu008@brin.go.id, [2]kevin.stekelorom@uphf.fr*

*Corresponding Author

Abstract

Some factors that need to be developed in the LoRaWAN satellite communication system are using LR-FHSS (Long Range-Frequency Hoppong Spread Spectrum) to increase resistance to frequency interference and jamming, with the technique of using a small bandwidth per channel and operating on the same spectrum. With LR-FHSS devices on Earth can communicate with satellites that have relatively many movements. LR-FHSS uses 137 kHz bandwidth which is divided per channel around 488 Hz, with coding rates of 1/3 and 2/3 and separately modulated headers and payloads, and hop distance is a range of 3-50 kHz. LR-FHSS implementation is for monitoring hard-to-reach areas such as oceans, mountains, deserts, and others, as well as logistics tracking and asset management. LR-FHSS LoRaWAN uses RP2-1.0.1 which is the LoRa Alliance standardization for satellite communication. This research shows the Frequency Hopping Pattern for each device, the graph shows that there are 3 devices, devices 1, 2, and 3, which are spread over the free frequency channel between 0.0 and 17.5 with time slots 0 to 90. CR 1 with Frequency Hopping produces the fastest Time-on-air (ms) of 2 ms, and CR 2/3 with Frequency Hopping 3 ms, this is the best setting to produce the fastest ToA.

Keywords: *LoRaWAN, Satellite Communication, LR-FHSS, Small Bandwidth, Frequency Interference*

1. Introduction

The long-range factor requires a method to be able to streamline the communication system built between Constellation satellites in Low Earth Orbit (LEO) and minimize data collisions due to high network density, spectral efficiency, and resistance to Doppler effects. LR-FHSS (Long Range-Frequency Hopping Spread Spectrum) can extend the capabilities of LoRaWAN on satellite communication. LR-FHSS technology uses a frequency hopping technique that follows a predetermined pseudo-random pattern [1,2,3]. The following is a simulation of LR-FHSS for LoRaWAN communication, this simulation shows how data transmission moves between channels and follows a Pseudo-random pattern.

Some things that need to be deepened in the use of LR-FHSS are the modulation techniques used and the characteristics of LR-FHSS in LPWAN satellite communications or this case LoRaWAN. Some of the characteristics are interference resistance, Spectral Efficiency, High Link Budget, Communication range, and low power consumption. As

ISSN: 2722-6050

for satellite communication systems, several companies have implemented LR-FHSS in their Satellite-based LPWAN telecommunication systems, including Lacuna Space, OrbComm Satellite, and Eutelsat IoT Constellation Satellite [4,5,6].

2. LR-FHSS for LoRaWAN Satellite

LR-FHSS combines spread spectrum technology with frequency hopping to create a reliable LoRaWAN Satellite based telecommunication system, for this reason, it is supported by the equation of LR-FHSS which can be developed comprehensively, as for the mathematical equation can be seen in equation 1 [7,8,9]. Where f_i is the carrier frequency for the i^{-th} hop, f_{based} is the base frequency used for satellite communications, typically 862 MHz for EU868 or 902 MHz for US915, while Δf is the frequency step (typically 25 kHz or 200 kHz), h_i is the i-th hopping value generated by the pseudo-random algorithm, while f_{range} is the available frequency range.

$$f_i = (f_{base} + \Delta f . h_i) mod\ f_{ranae} \tag{1}$$

$$h_i = (a . h_i - 1 + c)\ mod\ m \tag{2}$$

Equation 2 is the Linear Congruential Generator (LCG) function. Where *a* is the multiplier which is usually 1665425, while *c* is the increment whose value is 1013904223, while m is the modulus which is 2^32, while h_0 is the initial value (seed) which is derived with DevEUI and network parameters. In understanding LR-FHSS, the essential parameter is the Link Budget, where the Link Budget value for satellite communication can be obtained from equation 3 [10,11,12]. Where P_r is the received power at the satellite (dBm), P_t is the device transmission power (dBm), G_t is the device antenna gain (dBi), L_{fs} is the free space path loss (dB), L_a is the atmospheric loss (dB), G_r is the satellite receiver antenna gain (dBi), while L_m is the link margin and other losses (dB). The next calculation is as in equation 4, where Free Space Path Loss also affects determining the Quality of Service of LEO Satellite use LPWAN or LoRaWAN. Where d is the distance to the satellite in kilometers, and f is the carrier frequency in MHz.

$$P_r = P_t + G_t - L_{fs} - L_a + G_r - L_m \tag{3}$$

$$L_{fs} = 20 \log_{10}(d) + 20 \log_{10}(f) + 32.45 \tag{4}$$

Furthermore, Then in terms of the Doppler equation for a moving satellite can be shown in Equation 5. Where Δf_d is the Doppler shift (Hz), Vr is the relative speed of the satellite to the device (m/s), c is the speed of light (3x10^8 m/s), and fc is the carrier frequency (Hz). Moreover, the modulation or encoding used by LR-FHSS uses GMSK (Gaussian Minimum Shift Keying) which can be seen in equations 6 and 7 [13,14,15].

$$\Delta f_d = \frac{V_r}{c} . f_c \tag{5}$$

$$s(t) = Acos[2\pi f_c t + \phi(t)] \tag{6}$$

$$\phi(t) = 2\pi h \int_{-\infty}^{t} m(\tau) g(t-\tau) d\tau \tag{7}$$

Moreover, for the Coding Rate used in LoRa is CR 4/5 called CR1, 4/6 called CR2, 4/7 called CR3, and 4/8 called CR4. while for the effective bit rate formula (Rb) by considering the coding rate value, it can be formulated as the following equation 8:

$$Rb=SFx(BW/2\text{^}SF)x\ CR \tag{8}$$

3. Method

The LR-FHSS method on the LoRaWAN Satellite can be seen in Figure 1 [16,17]. In the flowchart, several parameters accompany each component such as End Devices, LR-FHSS Transmission, Satellite Reception, Network Server, Application Server, and Downlink Path [18].

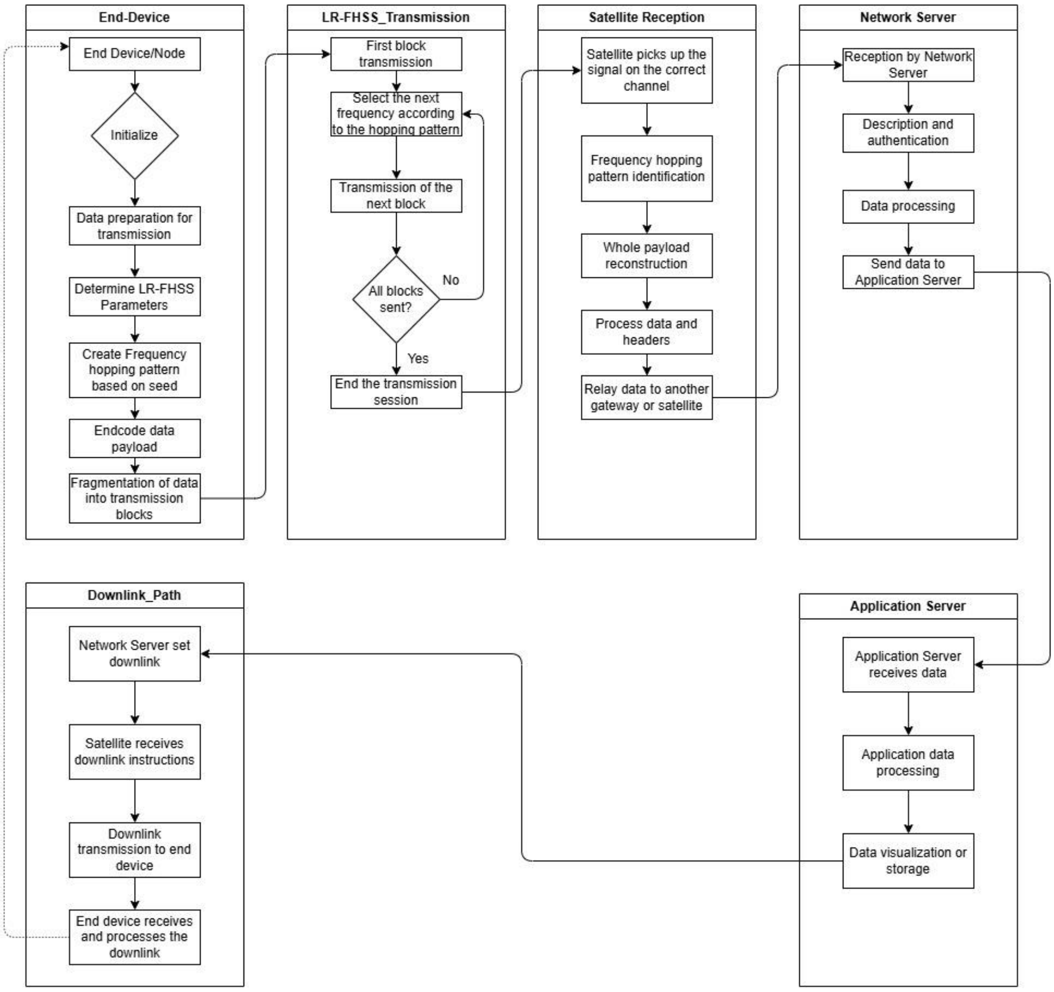

Figure 1. Flowchart LR-FHSS untuk LoRaWAN Satellite Communication

Figure 1 shows a flowchart diagram of a satellite communication system with six main parts: End Device, which shows the process of preparing data for transmission, including creating frequency hopping patterns, encoding data, and breaking data into transmission blocks, and LR-FHSS Transmission [19,20], which illustrates the transmission process with a decision flow for block handling. If the block is still to be transmitted, the system will continue the transmission; otherwise, the system will end the transmission session. The satellite Reception System is responsible for describing how satellites receive signals, identify patterns, process data, and forward it to gateways or other satellites. Then Network Server Shows the reception, decryption, processing, and delivery of data to the Application Server. Then Downlink_Path which Describes the return path from the Network Server to the End Device via satellite. And finally, the Application Server whose task is to describe the reception, processing, and visualization or storage of data. In detail, the core of the Flowchart is the uplink and downlink process on LoRaWAN Satellite communication with the LR-FHSS mechanism.

4. Result and Analysis

Furthermore, in Figures 2a, 2b, 2c, 2d, & 2e, Gaussian Minimum Shift Keying (GMSK) modulation with Frequency Hopping Spread Spectrum (LR-FHSS) capability is implemented. GMSK modulation converts binary data (0s and 1s) to NRZ format (-1s and 1s), applies a Gaussian filter to smooth the transition, integrates the filtered signal to obtain phase information, and generates I and Q components based on phase. There is also Frequency Hopping which consists of random frequency hopping patterns, applying frequency hopping at specified intervals, and integrating the frequency offset into the signal phase. In Visualization, there are Time-domain plots of bit sequences, NRZ data, and filtered signals, Frequency domain analysis showing frequency hopping patterns, a Spectrogram showing frequency changes over time, an I/Q constellation diagram, and a Comparison of transmitted and received bits. In Receiver Simulation, there is a basic coherent receiver implementation, and calculating the bit error rate (BER).

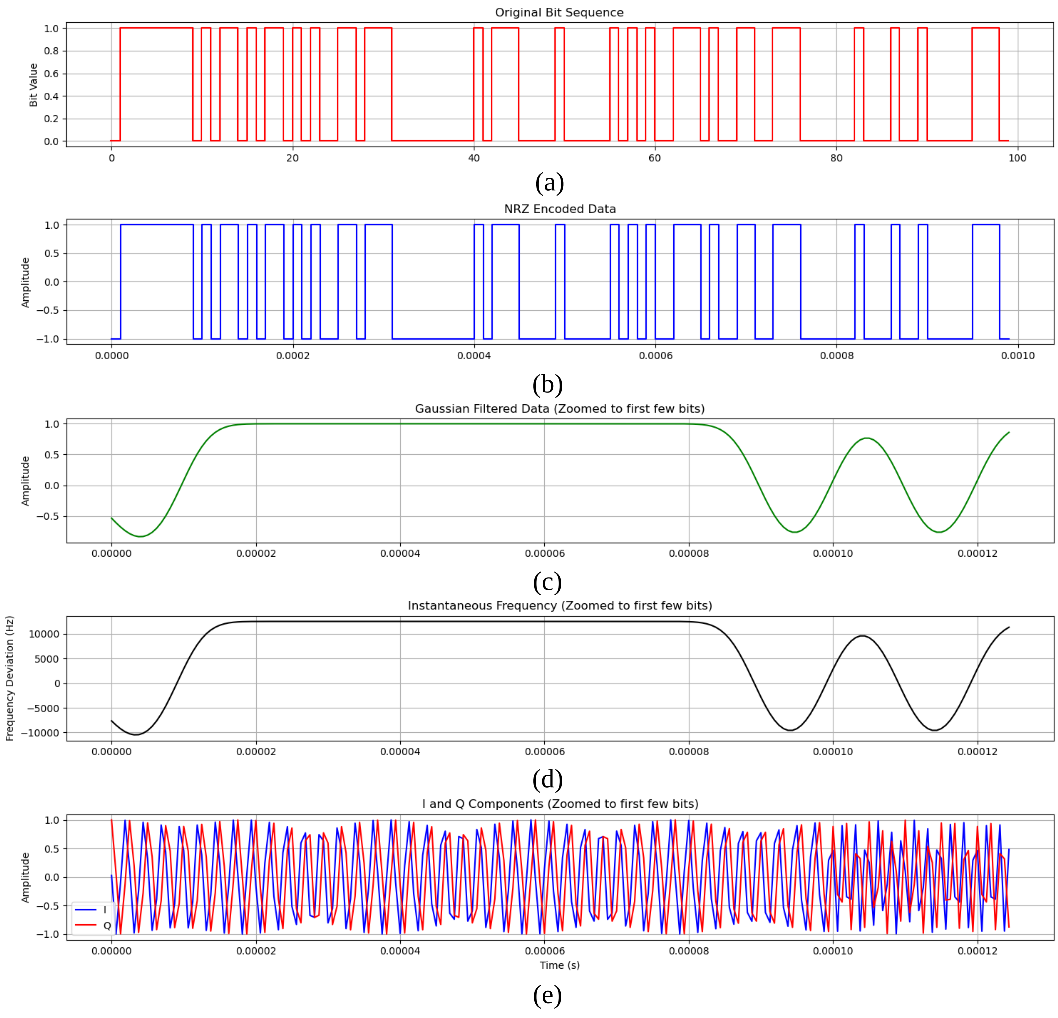

Figure 2. (a) Original bit sequence (b) NRZ Encoded data (c) Gaussian Filtered Data (d) Instantaneous Frequency (e) I and Q Components

Figure 3a shows the spectrogram of a GMSK (Gaussian Minimum Shift Keying) signal with frequency hopping. This spectrogram shows the frequency of the signal changing over time. The parameters observed in the following spectrogram are Frequency Hopping Pattern, Hop Intervals, in this spectrogram using 0.001 seconds per regular interval, then Channel Distribution, Power Concentration, and Gaussian Shaping.

(a)

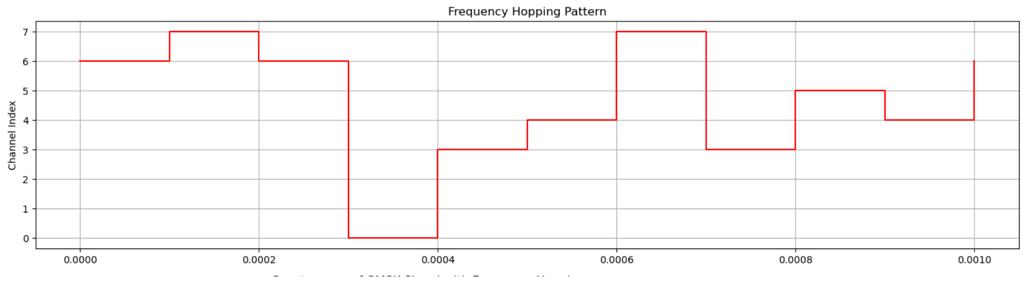

(b)

Figure 3. (a) Spectogram of GMSK Signal with Frequency Hopping (b) Frequency Hopping Pattern

Figure 3 b shows the spectrum of the GMSK Signal with Frequency Hopping and Frequency Hopping Patterns. Figure 3b shows the skip pattern used in the LR-FHSS system, there are several components, the horizontal part is Time (seconds), ranging from 0 to 0.009 seconds, while the vertical is the channel index 0-7 which indicates different frequency channels. While the red color line shows the frequency skip sequence from Time to Time, while Figure 4 is the I/Q Constellation Diagram, Figure 4 shows that the GMSK modulation is working correctly, this information is shown in the phase transition, not at a specific constellation point, the signal changes continuously and forms a circle. The constant phase envelope is very beneficial for efficient power amplifier operation without any distortion. While Figure 5 is the Bit Comparison between Transmitted Bits and Received Bits.

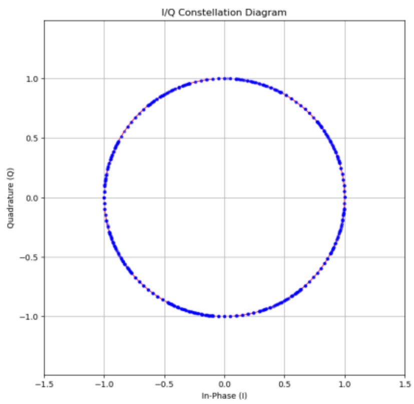

Figure 4. I/Q Constellation Diagram

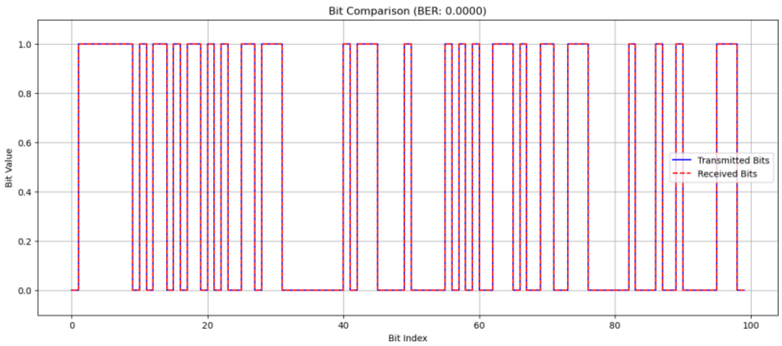

Figure 5. Bit Comparison

The LR-FHSS Signal in Time Domain is shown in Figure 6a, while the LR-FHSS Signal Spectogram is shown in Figure 6b. Figure 7a is the Frequency Hopping Pattern, showing the comparison between Channel Index and Hop Number, and 7b is the Link Budget vs Distance showing the SNR (dB) value decreasing with increasing distance (km), and also the Received Power (dBm) decreasing with increasing distance.

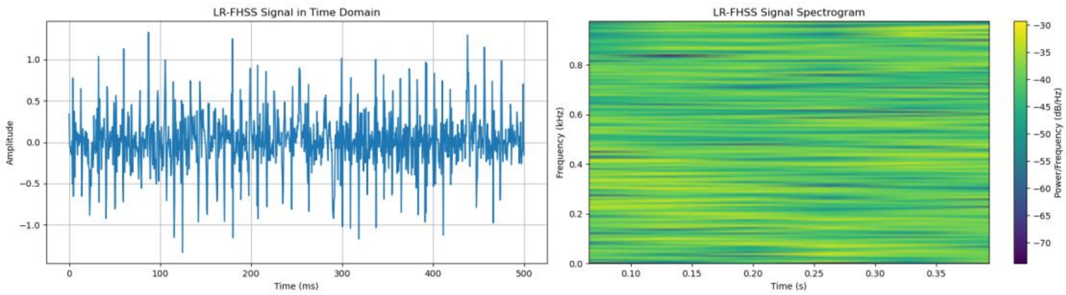

(a) (b)

Figure 6. (a) LR-FHSS Signal in Time Domain, (b) LR-FHSS Signal Spectogram

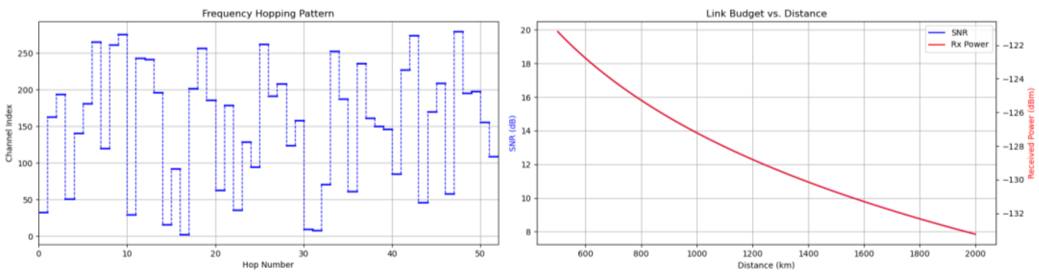

(a) (b)

Figure 7. (a) Frequency Hopping Pattern, (b) Link Budget vs Distance

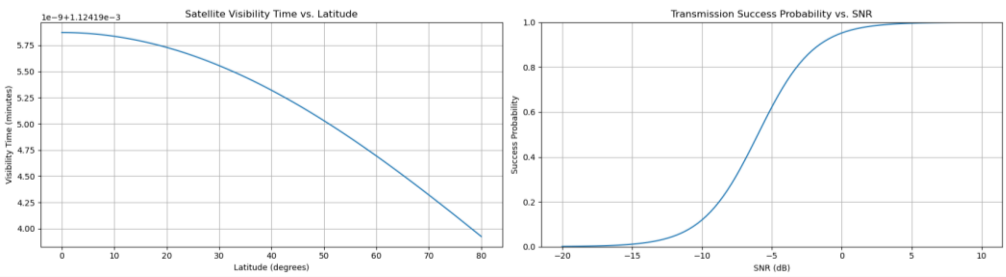

(a) (b)

Figure 8. (a) Satellite Visibility Time vs. Latitude, (b) Transmission Success Probability vs. SNR

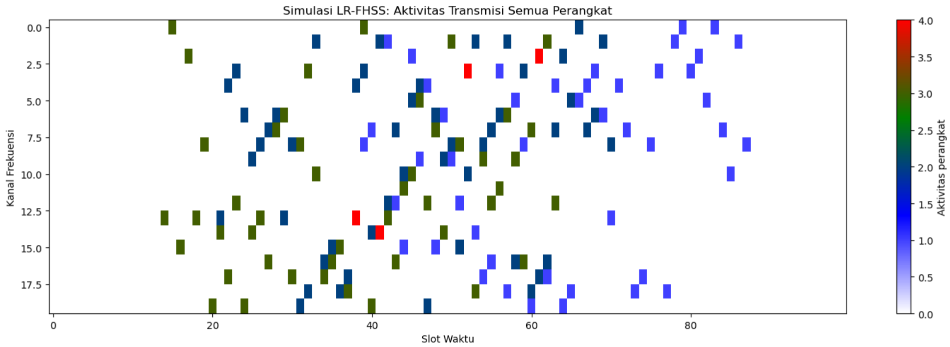

Figure 9. LR-FHSS Simulation Results with the transmission activity of all devices

Figure 8a shows Satellite Visibility Time vs Latitude, while Figure 8b shows Success Probability versus SNR (dB). Figure 9 shows the LR-FHSS Simulation Result which shows the Transmission Activity of all devices, this is a comparison between the Frequency Channel and Time Slot, the intensity or number of devices starts with white color which is 0.0 to red color with a value of 4.0 which indicates dense device activity in the free frequency channel which is in 0.0 to 17.5. Moreover, Figure 10 shows the Frequency Hopping Pattern for each device, the graph shows that there are 3 devices, namely devices 1, 2, and 3, which are spread over the free frequency channel between 0.0 and 17.5 with time slots 0 to 90. Finally, Figure 11 shows the Distribution of Canal usage Frequency, this is a comparison between the amount of usage and the frequency channels used.

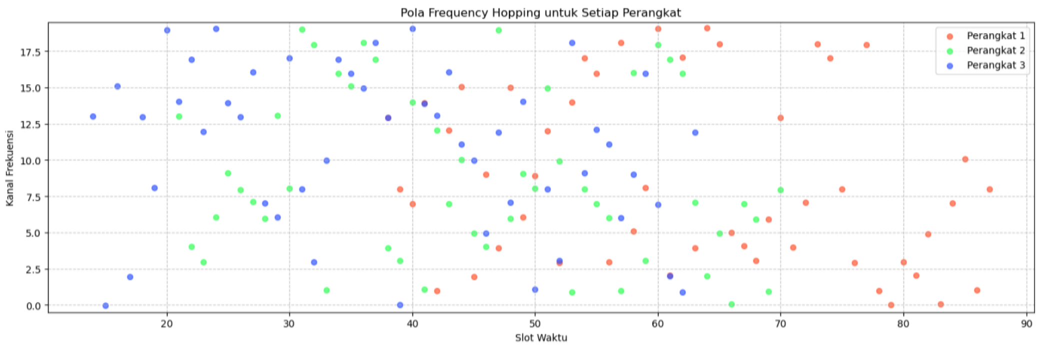

Figure 10. Frequency Hopping pattern for all devices

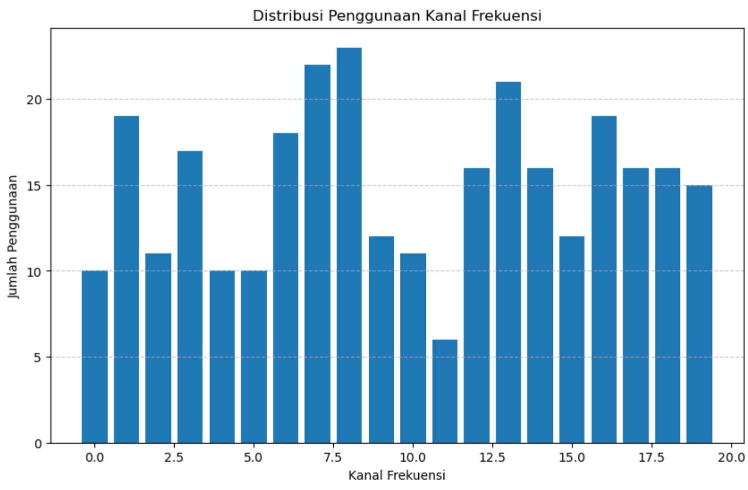

Figure 11. Distribution of canal usage Frequency

Figure 11 shows a visualization to analyze the efficiency of frequency allocation in LR-FHSS systems. The presence of a somewhat uneven distribution is normal and often beneficial in frequency hopping systems, as it allows the system to select channels with better performance while still maintaining enough randomness to provide resilience to interference and congestion.

Furthermore, In the experiment using LR-FHSS, there are several elements, namely Frequency Hopping, Coding Rate consisting of CR 1/3 is high redundancy, low data rate, and resistance to noise, CR2/3 is medium redundancy, medium data rate, and CR1 is without redundancy, high data rate, and less resistant to noise. The next element is the satellite channel effect which consists of path loss based on satellite distance and Gaussian noise based on SNR level. The next element is the Performance Matrix for Packet Reception Rate (PRR), Bit Error Rate (BER), Time-on-Air (ToA), and Data Rate. Figure 12 is a comparison of Packet Reception Rate with the comparison of CR 1/3 with Frequency Hopping CR 1/3 without Frequency Hopping CR 2/3 with Frequency Hopping, and CR 1 with Frequency Hopping compared to Packet Reception Rate. The Bit Error Rate comparison is shown in Figure 13, with the comparison of CR 1/3 with Frequency Hopping, CR 1/3 without Frequency Hopping, CR 2/3 with Frequency Hopping, and CR 1 with Frequency Hopping. Figure 13 shows the comparison of Bit Error Rate vs SNR (dB), with BER values in the range of 0.4, 0.5, and 0.6.

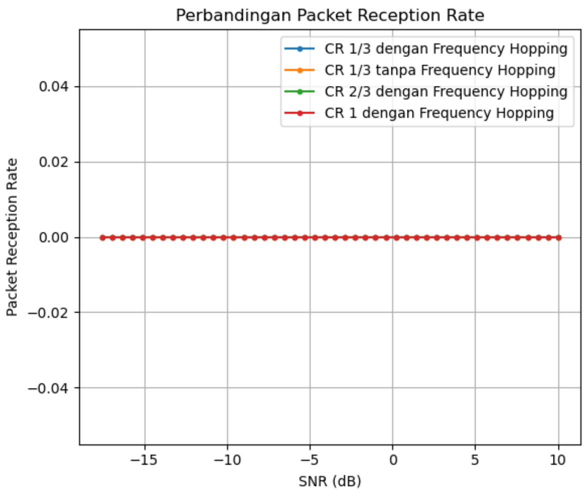

Figure 12. Comparison of Package Acceptance Rate

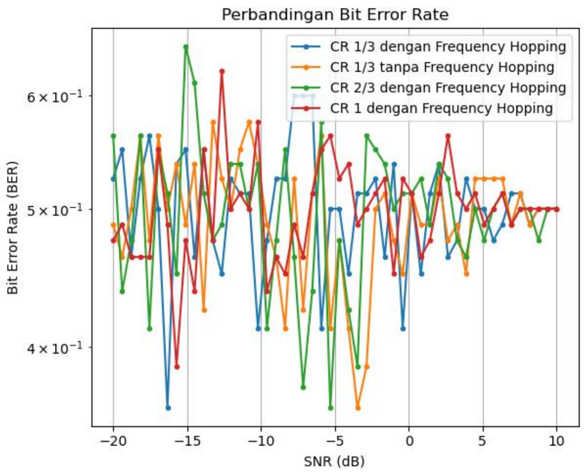

Figure 13. Bit Error Rate Comparison

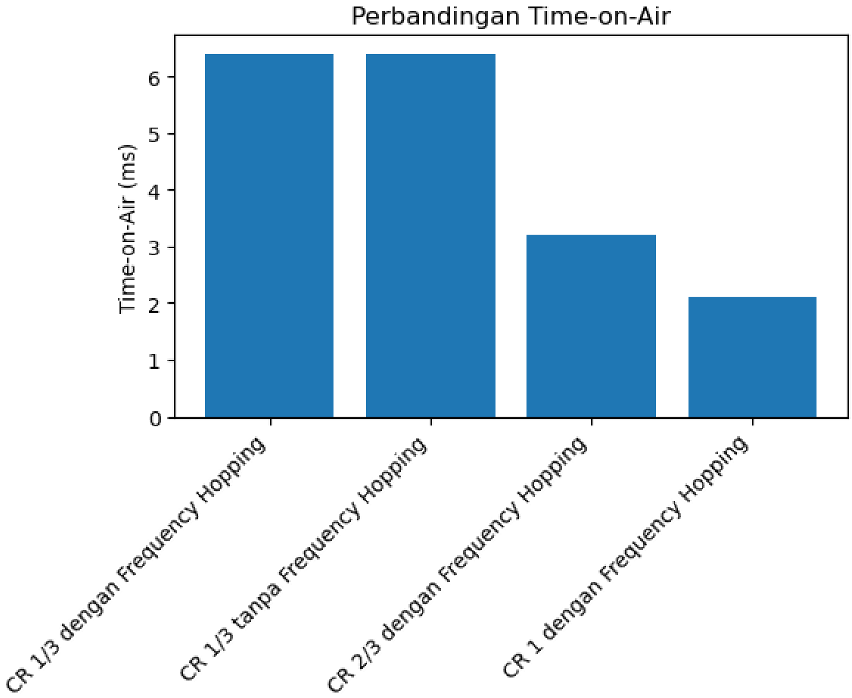

Figure 14. Time-on-Air Comparison

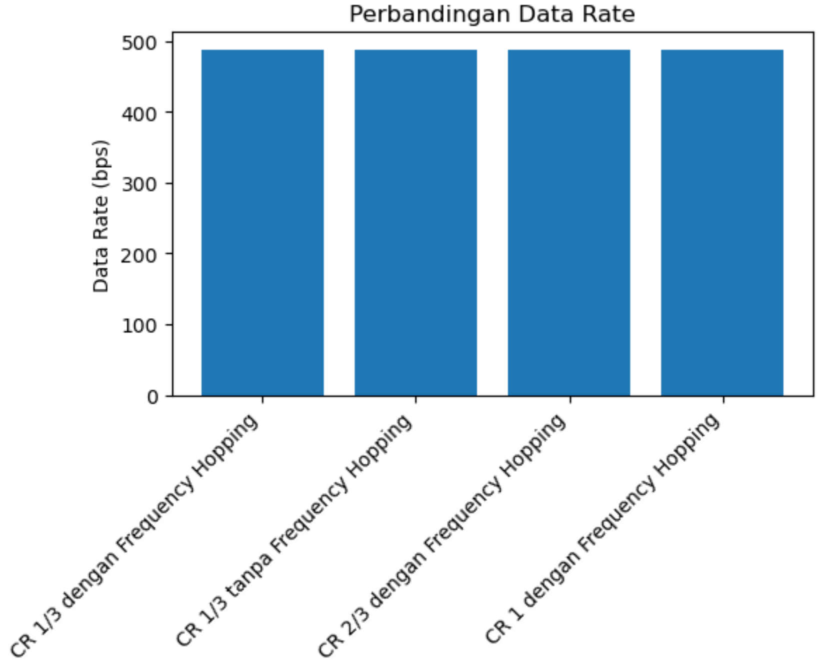

Figure 15. Data Rate Comparison

Figure 14 is a Time-on-air comparison, there are four parameters namely CR 1/3 with Frequency Hopping, CR 1/3 without Frequency Hopping, CR 2/3 with Frequency Hopping, and CR1 with Frequency Hopping, with each having a different Time-on-air (ms), can be seen that CR 1 has the fastest Time-on-air at 2 ms, while CR 2/3 with frequency hopping with ToA 3 ms. While CR 1/3 with no frequency hopping is the same at ToA 6 ms. About Data Rate, there are four criteria for using CR, namely 1/3 CR 2/3, and CR 1. From all CR settings, the data rate is 500 bps.

5. Conclusions

LR-FHSS (Long Range Frequency Hopping Spread Spectrum) is a comprehensive advancement in the field of satellite communication based on LoRaWAN. LR-FHSS supports the development of satellite-based Internet of Things (IoT) technology for wider and more efficient distance development. By using the LR-FHSS mechanism, it is possible to communicate multi-point more effectively. By using LR-FHSS it is possible to increase spectrum efficiency more optimally than with traditional LoRa modulation. Increased network capacity is essential for satellite constellations that must serve the entire vast area of the earth with limited spectrum resources. In addition, LR-FHSS can increase interference resistance.

LR-FHSS may be able to increase interference resistance, by performing fast jumps by crossing multiple frequency channels, LR-FHSS is also able to provide strong protection against interference due to narrow band, signal interference, and frequency selective fading as Radio Frequency is unpredictable in terms of interference and also signal Attenuation Loss. The next benefits of LR-FHSS are in addition to wide coverage, reduced power consumption, and flexibility where LR-FHSS follows the channel distribution and frequency regulations in the region, continent, or country, as well as being able to be integrated with LoRaWAN infrastructure that can replace ground infrastructure or terrestrial areas into LoRaWAN Satellite with a wider range of coverage. The Frequency Hopping Pattern for each device with three devices, devices 1, 2, and 3, which are spread over the free frequency channel between 0.0 and 17.5 with time slots 0 to 90. The point of LR-FHSS is to select channels with better performance while still maintaining sufficient randomness and providing robustness against interference and congestion. CR 1 with Frequency Hopping produces the fastest Time-on-air (ms) of 2 ms, and CR 2/3 with Frequency Hopping 3 ms, this is the best setting to produce the fastest ToA.

Acknowledgments

Thanks to the entire team who have worked hard in completing this research, in the future, I hope BRIN Telecommunication Research Center can collaborate with Lacuna Space to develop LoRaWAN Satellite communication for the growth of the Internet of Things (IoT) in the future.

References.

[1] A. Maleki, H. H. Nguyen, E. Bedeer and R. Barton, "Outage Probability Analysis of LR-FHSS and D2D-Aided LR-FHSS Protocols in Shadowed-Rice Fading Direct-to-Satellite IoT Networks," in IEEE Internet of Things Journal, vol. 11, no. 6, pp. 11101-11116, 15 March15, 2024, doi: 10.1109/JIOT.2023.3329361.

[2] J. M. de Souza Sant'Ana, A. Hoeller, H. Alves and R. D. Souza, "LR-FHSS-Sim: A Discrete-Event Simulator for LR-FHSS Networks," 2024 Joint European Conference on Networks and Communications & 6G Summit (EuCNC/6G Summit), Antwerp, Belgium, 2024, pp. 700-705, doi: 10.1109/EuCNC/6GSummit60053.2024.10597000

[3] S. Rathi and S. S. Borkotoky, "Message Replication for Improving Reliability of LR-FHSS Direct-to-Satellite IoT," 2024 IEEE International Conference on Advanced Networks and Telecommunications Systems (ANTS), Guwahati, India, 2024, pp. 1-6, doi: 10.1109/ANTS63515.2024.10898895.

[4] M. A. Ullah, K. Mikhaylov and H. Alves, "Analysis and Simulation of LoRaWAN LR-FHSS for Direct-to-Satellite Scenario," in IEEE Wireless Communications Letters, vol. 11, no. 3, pp. 548-552, March 2022, doi: 10.1109/LWC.2021.3135984.

[5] J. M. de Souza Sant'Ana, O. d. S. Neto, A. Hoeller, J. L. Rebelatto, R. D. Souza and H. Alves, "Asynchronous Contention Resolution-Aided ALOHA in LR-FHSS Networks," in IEEE Internet of Things Journal, vol. 11, no. 9, pp. 16684-16692, 1 May1, 2024, doi: 10.1109/JIOT.2024.3355709.

[6] M. A. Ben Temim, G. Ferré and O. Seller, "An LR-FHSS Receiver for a Massive IoT Connectivity," 2023 IEEE 34th Annual International Symposium on Personal, Indoor and Mobile Radio

Communications (PIMRC), Toronto, ON, Canada, 2023, pp. 1-6, doi: 10.1109/PIMRC56721.2023.10293878.

[7] F. Zhang, F. Yu, X. Zheng, L. Liu and H. Ma, "DFH: Improving the Reliability of LR-FHSS via Dynamic Frequency Hopping," 2023 IEEE 31st International Conference on Network Protocols (ICNP), Reykjavik, Iceland, 2023, pp. 1-12, doi: 10.1109/ICNP59255.2023.10355600.

[8] A. Maleki, H. H. Nguyen and R. Barton, "Outage Probability Analysis of LR-FHSS in Satellite IoT Networks," in IEEE Communications Letters, vol. 27, no. 3, pp. 946-950, March 2023, doi: 10.1109/LCOMM.2022.3233524

[9] A. Maleki, E. Bedeer and R. Barton, "Performance Evaluation and Low-Complexity Detection of the PHY Modulation of LR-FHSS Transmission in IoT Networks," 2024 IEEE 99th Vehicular Technology Conference (VTC2024-Spring), Singapore, Singapore, 2024, pp. 1-7, doi: 10.1109/VTC2024-Spring62846.2024.10683565.

[10] D. N. Knop, J. L. Rebelatto and R. D. Souza, "LR-FHSS With Network-Coded Header Replication," in IEEE Transactions on Vehicular Technology, vol. 73, no. 6, pp. 9066-9070, June 2024, doi: 10.1109/TVT.2024.3350635.

[11] J. d. A. Farhat, J. Michel de Souza Sant'Ana, J. L. Rebelatto, N. H. Mahmood, G. Pasolini and R. D. Souza, "Probabilistic Allocation of Payload Code Rate and Header Copies in LR-FHSS Networks," in IEEE Access, vol. 13, pp. 30010-30020, 2025, doi: 10.1109/ACCESS.2025.3541407.

[12] G. Boquet, P. Tuset-Peiró, F. Adelantado, T. Watteyne and X. Vilajosana, "LR-FHSS: Overview and Performance Analysis," in IEEE Communications Magazine, vol. 59, no. 3, pp. 30-36, March 2021, doi: 10.1109/MCOM.001.2000627

[13] G. Álvarez, J. A. Fraire, K. A. Hassan, S. Céspedes and D. Pesch, "Uplink Transmission Policies for LoRa-Based Direct-to-Satellite IoT," in IEEE Access, vol. 10, pp. 72687-72701, 2022, doi: 10.1109/ACCESS.2022.3189647.

[14] C. D. Gedara, M. D. Khattak, M. A. Ullah and K. Mikhaylov, "Direct-to-Satellite Connectivity for IoT: Overview and Potential of Reduced Capability (RedCap)," 2023 IEEE 9th World Forum on Internet of Things (WF-IoT), Aveiro, Portugal, 2023, pp. 1-8, doi: 10.1109/WF-IoT58464.2023.10539387.

[15] D. Wang, A. Elzanaty and M. -S. Alouini, "Coded Frequency Hopping for Direct-to-Satellite IoT Systems: Design and Analysis," in IEEE Internet of Things Journal, vol. 11, no. 22, pp. 36335-36349, 15 Nov.15, 2024, doi: 10.1109/JIOT.2024.3404093.

[16] E. Testi and E. Paolini, "Packet Collision Probability of Direct-to-Satellite IoT Systems," in IEEE Internet of Things Journal, vol. 12, no. 2, pp. 1843-1855, 15 Jan.15, 2025, doi: 10.1109/JIOT.2024.3470113

[17] K. Lin, M. A. Ullah, H. Alves, K. Mikhaylov and T. Hao, "Subterranean mMTC in Remote Areas: Underground-to-Satellite Connectivity Approach," in IEEE Communications Magazine, vol. 61, no. 5, pp. 136-142, May 2023, doi: 10.1109/MCOM.002.2200194

[18] H. E. Susilo and J. Suryana, "Research on LPWAN Direct to Satellite IoT: A Survey Technology and Performance on LEO Satellite," 2023 29th International Conference on Telecommunications (ICT), Toba, Indonesia, 2023, pp. 1-7, doi: 10.1109/ICT60153.2023.10374072.

[19] Maldonado, D. et.al. 2025. Enhanced LR-FHSS receiver for headerless frame recovery in space–terrestrial integrated IoT networks. Computer Networks. Volume 257, February 2025, 111018. doi. 10.1016/j.comnet.2024.111018

[20] Sanchez-Vital, R.; Casals, L.; Heer-Salva, B.; Vidal, R.; Gomez, C.; Garcia-Villegas, E. Energy Performance of LR-FHSS: Analysis and Evaluation. Sensors 2024, 24, 5770. https://doi.org/10.3390/s24175770